한국환경과학회지 제16권(제1호), 1~8, 2007
Journal of the Environmental Sciences

Atmospheric Photochemistry in Low- and High-NO_X Regimes

Do-Yong Kim, Satoshi Soda*, Akira Kondo* and Jai-Ho Oh**
Center for Atmospheric Sciences & Earthquake Research, korea Meteorological Administration, Busan 608-737, Korea
**Graduate School of Engineering, Osaka University, Osaka 565-0871, Japan*
***Department of Environmental Atmospheric Sciences, Pukyong National University, Busan 608-737, Korea*
(Manuscript received 1 August, 2006; accepted 26 December, 2006)

Atmospheric photochemistry of O_3-NO_X-RH were considered theoretically, to clarify the reasons for the different trends of between the formation of photochemical oxidants (O_X) and its primary pollutants for the Low- and High-NO_X regimes. Equations of OH, HO_2, and production of ozone (O_3) as a function of nitrogen oxides (NO_X) and reactive hydrocarbons (RH) were represented in this study. For the Low-NO_X regime, HO_2 radical is proportional to RH but independent of NO_X. OH radical is proportional to NO_X but inversely-proportional to RH. O_3 production is proportional to NO_X but has a weak dependence on RH. For the High-NO_X regime, OH and HO_2 radicals concentrations and O_3 production are proportional to RH but inversely-proportional to NO_X. In addition, the Osaka Bay and surrounding areas of Japan were evaluated with the mass balance of odd-hydrogen radicals (Odd-H) using CBM-IV photochemical mechanism, in order to distinguish the Low- and High-NO_X regimes. The Harima area (emission ratio, RH/NO_X = 6.1) was classified to the Low-NO_X regime. The Hanshin area (RH/NO_X = 3.5) and Osaka area (RH/NO_X = 4.3) were classified to the High-NO_X regime.

Key Words : Photochemical oxidants (O_X), Nitrogen oxides (NO_X), Reactive hydrocarbons (RH), Low-NO_X regime, High-NO_X regime

1. Introduction

It is considered significantly today that photochemical oxidants (O_X) such as ozone (O_3) and peroxy-acyl-nitrate (PAN) are generated by complicated chemical reactions[1~4] involving solar ultraviolet rays and its emission of primary pollutants such as nitrogen oxides (NO_X) and reactive hydrocarbons (RH) in the atmosphere. A great number of individual chemical reactions have been identified in the formation of photochemical oxidants, and the mechanisms involved in the generation of these substances have not yet been thoroughly worked out. Specifically, O_3 occupies the most of photochemical oxidants, and has been considered in many studies in recent years in order to reduce photochemical O_X. O_3 in the stratospheric protects the Earth's surface from high levels of biologically damaging ultraviolet radiation, which is known to be a significant risk factor for skin cancers, eye cataracts, and immune system suppression. However, surface O_3 as one of the photochemical O_X causes photochemical smog, and has effects on human health and plants, such as bronchitis, asthma, leaf injury, crop reduction. This surface photochemical O_3 is also one of the most remarkable pollutants today, and high level O_3 which exceeds twice as high as the environmental standard is often observed in the big urban areas[5~7]. Therefore, it is necessary to decreasing photochemical O_3 for improvement of air quality.

The relationship between photochemical O_3 and its primary pollutants such as NO_X and RH has been a focus of many studies in recent years in order to find ways to decrease O_3 in the atmosphere. However, it has been difficult to determine whether O_3 production during specific events is associated with the chemistry of Low- and High-NO_X regimes[8~11]. The chemistry of Low-NO_X regime, also known as the RH-rich system, appears in polluted rural and small urban areas with high RH/NO_X emission ratios where small artifi-

Corresponding Author : Do-Yong Kim, Center for Atmospheric Sciences & Earthquake Research, Korea Meteorological Administration, Busan 608-737, Korea
Phone: +82-51-620-6254
E-mail: dykim@cater.re.kr

cial NO_X emission sources and high levels of biogenic hydrocarbon from forests exist. The chemistry of High-NO_X regime, also called the NO_X-rich system, appears in urban areas with low RH/NO_X emission ratios in which large artificial NO_X emission sources are contained[12~14]. The different results for the Low- and High-NO_X regimes from their studies on the relationship between photochemical O_3 and primary pollutants such as NO_X and RH were reported, due to the meteorological and geographical dependence of the O_3-NO_X-RH chemistry in objected areas. Generally, for the Low-NO_X regime, the reduction in NO_X emission was effective in decreasing O_3 level. For the High-NO_X regime, the reduction in RH emission was very effective in decreasing O_3 level, and reduction in NO_X emission led to an increase in O_3 concentration above its uncontrolled value.

In this study, the atmospheric photochemistry of O_3-NO_X-RH were considered theoretically, to clarify the reasons for the different trends of between photochemical O_3 and its primary pollutants for the Low- and High-NO_X regimes. In addition, the Osaka Bay and surrounding areas of Japan were evaluated with the mass balance of odd-hydrogen radicals (Odd-H) using CBM-IV (Carbon Bond Mechanism IV) photochemical mechanism by Gery *et al.*[3], in order to distinguish the Low- and High-NO_X regimes.

2. General Photochemistry

The photochemical oxidants such as O_3 and PAN are generated by complicated chemical reactions involving solar ultraviolet rays and its emission of primary pollutants such as NO_X and RH in the atmosphere. O_3 production results from photolysis of NO_2, reaction (R1), when an oxygen atom generated by the photolysis rapidly combines with molecular oxygen (O_2) to produce O_3.

(R1) $NO_2 + h\nu + O_2 \rightarrow NO + O_3$

NO_2 production occurs by reaction of RO_2 or HO_2 with NO, reactions (R4) and (R5). RO_2 and HO_2 are produced by reactions of OH with RH and CO, respectively (reactions (R2) and (R3)). The oxidation pathways for RH discussed in more detail by Atkinson[15]. HO_2 is also produced by the reaction of RO_2 with NO, reaction (R4). Thus, the major photochemical pathway for O_3 production by reaction (R1) is through NO_2 formation via reaction (R5). In (R4), RCHO represents intermediate organic species, typically including aldehydes and ketones. Here, RH in reaction (R2) was defined as the sum of RH species. For example, the species of RH important in photochemical reactions are classified as PAR, OLE, ETH, TOL, or XYL on the basis of the similarity of their chemical bonding in CBM-IV[3] as a popular photochemical reaction mechanism. PAR stands for paraffin species with a carbon single bond, OLE for olefin species with a carbon double bond, ETH and TOL for ethene and toluene species with mono-alkyl-benzene groups, respectively, and XYL for xylene species with di- or tri-alkyl-benzene groups.

(R2) $RH + OH + O_2 \rightarrow RO_2 + H_2O$
(R3) $CO + OH + O_2 \rightarrow HO_2 + CO_2$
(R4) $RO_2 + NO + O_2 \rightarrow RCHO + HO_2 + NO_2$
(R5) $HO_2 + NO \rightarrow OH + NO_2$

The major photochemical pathways for removal of O_3 are photolysis, reaction (R6), and reactions with NO and HO_2, reactions (R7) and (R8). Also, formation of nitric acid (HNO_3), reaction (R9), is important for removal of O_3, because it involves consumption of OH radical, which produces RO_2 and HO_2 in the chain-terminating steps in reactions (R2) and (R3).

(R6) $O_3 + h\nu + H_2O \rightarrow 2OH + O_2$
(R7) $NO + O_3 \rightarrow NO_2 + O_2$
(R8) $HO_2 + O_3 \rightarrow OH + 2O_2$
(R9) $OH + NO_2 \rightarrow HNO_3$

The photolysis of formaldehyde (HCHO) and RCHO produces HO_2, reaction (R10), and RO_2, reaction (R11), respectively.

(R10) $HCHO + h\nu + 2O_2 \rightarrow 2HO_2 + CO$
(R11) $RCHO + h\nu + 2O_2 \rightarrow RO_2 + HO_2 + CO$

In this study, it is used that a definition of odd-hydrogen radicals (Odd-H) includes RO_2 and RCO_3 species (e.g., CH_3O_2, CH_3CO_3), in addition to OH and HO_2[16]. Major sinks for Odd-Hinclude formation of hydrogen peroxide (H_2O_2), higher peroxides (ROOH), and HNO_3 by reactions (R12), (R13), and (R9), respectively.

(R12) $HO_2 + HO_2 \rightarrow H_2O_2 + O_2$

(R13) $RO_2 + HO_2 \rightarrow ROOH + O_2$

Formation and sink processes for PAN occur by reactions (R14) and (R15), respectively. These PAN mechanisms also represent sink and formation reactions for peroxyacyl radical (RCO_3). However, the main formation and sink processes for RCO_3 occur by reactions (R16) and (R17), respectively.

(R14) $RCO_3 + NO_2 \rightarrow PAN$
(R15) $PAN \rightarrow RCO_3 + NO_2$
(R16) $RCHO + OH + O_2 \rightarrow RCO_3 + H_2O$
(R17) $RCO_3 + NO + O_2 \rightarrow RO_2 + NO_2 + CO_2$

3. Theoretical Considerations of photochemistry

3.1. Theoretical Considerations

The theoretical considerations for the photochemistry of oxidants based on Sillman *et al.*[11], Milford *et al.*[12], and Sillman[14] are described. Several common terms such as OH radical, peroxy radicals (RO_2, HO_2, and RCO_3), PAN, and O_3 production are also presented and defined here.

Fig. 1 shows the schematic diagram for O_3-NO_X-RH photochemistry and radical reactions cycles based on above reactions (R1)~(R17). Odd-H (represented by gray squares) plays a key role in the photochemical mechanism. The sink of PAN and photolysis of O_3, HCHO, and RCHO produce Odd-H (represented by double circles) by reactions (R15), (R6), (R10), and (R11), respectively. The sinks of Odd-H (represented by diamonds) include formation of HNO_3, H_2O_2, ROOH, and PAN by reactions (R9), (R12), (R13), and (R14), respectively. Therefore, the Odd-H balance is expressed as follows in Eq. (1), where, k_i represents the rate constant for each reaction.

$$2k_6[O_3]+2k_{10}[HCHO]+2k_{11}[RCHO]+k_{15}[PAN] \\ =k_9[OH][NO_2]+2k_{12}[HO_2]^2+2k_{13}[RO_2][HO_2] \\ +k_{14}[RCO_3][NO_2] \quad (1)$$

Reaction of RCHO with OH (R16) represents its major sink, and photolysis (R10) provides an additional sink for HCHO. Consequently, the steady state concentration of RCHO is proportional to RH but independent of OH, and HCHO concentration is also proportional to RH but depends weakly on OH[11]. Therefore, Odd-H production by photolysis of HCHO and RCHO in Eq. (1) are represented as follows:

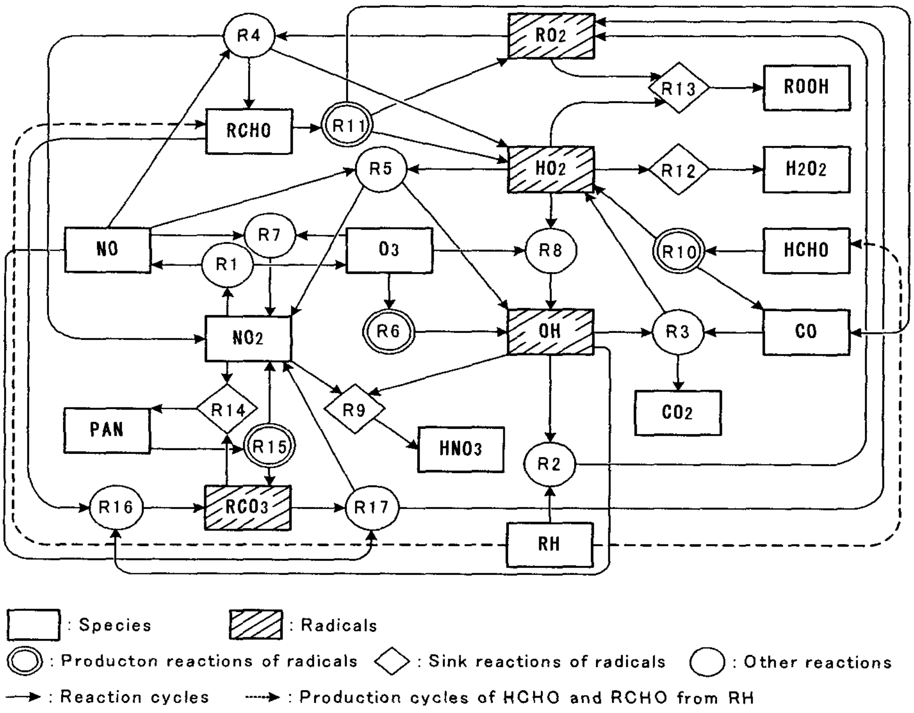

Fig. 1. Schematic diagram of O_3-NO_X-RH and radical reaction cycles involved in the production and sink of photochemical O_3.

$$k_{10}[HCHO] = A'[OH][RH] \quad (2)$$

$$k_{11}[RCHO] = B'[RH] \quad (3)$$

In typical summer conditions, the lifetime of PAN is short, and PAN may be assumed to be in steady state[11,17]: the reaction rate of PAN production (R14) must be equal to that of PAN sink (R15). Thus, PAN is represented as follows:

$$[PAN] = \frac{k_{14}}{k_{15}}[RCO_3][NO_2] \quad (4)$$

Hence, Eq. (1) can be rewritten as follows using Eq. (2), (3), and (4).

$$2k_6[O_3] + A[OH][RH] + B[RH] = k_9[OH][NO_2] + 2k_{12}[HO_2]^2 + 2k_{13}[RO_2][HO_2] \quad (5)$$

In Eq. (5), the A (=2 A') and B (=2 B') terms account for the sources of Odd-H from photolysis of HCHO and RCHO, respectively.

Peroxy radicals (HO_2, RO_2) play a key role in O_3 production. Production of HO_2 radical mainly occurs by reactions of CO with OH, reaction (R3), and NO with RO_2, reaction (R4). The RO_2 radical production mainly occurs by reaction of RH with OH, reaction (R2). In this major mechanism of O_3 production, the peroxy radical balance is expressed as follows:

$$k_2[OH][RH] + k_3[CO][OH] = k_5[HO_2][NO] \quad (6)$$

Here, k_2 is the concentration-weighted mean rate for reaction of OH with the ambient mix of RH. OH concentration, as implied by Eq. (6), can be represented as follows:

$$[OH] = \frac{k_5[HO_2][NO]}{k_2[RH] + k_3[CO]} \quad (7)$$

O_3 production rate, $P(O_3)$ is proportional to the production of the peroxy radicals in reactions (R2) and (R3), can be represented by Eq. (8). Eq. (8) shows that production of O_3 depends significantly on RH and NO_X involving Odd-H radicals cycle.

$$P(O_3) \sim [OH](k_2[RH] + k_3[CO]) \approx k_5[HO_2][NO] \quad (8)$$

The chemistry of PAN may have a major effect on NO_X levels and on O_3 production. RCO_3 balance in the steady state[17] can be also be written as:

$$k_{15}[PAN] + k_{16}[RCHO][OH] = k_{14}[RCO_3][NO_2] + k_{17}[RCO_3][NO] \quad (9)$$

Here, Eq. (9) can be rewritten as follows using Eq. (4) in steady state.

$$[RCO_3] = \frac{k_{16}}{k_{17}} \cdot \frac{[RCHO][OH]}{[NO]} \quad (10)$$

Also, the steady state relationship for O_3, NO and NO_2[11] is

$$\frac{[NO_2]}{[NO]} = \frac{k_7}{k_1}[O_3] \quad (11)$$

Hence, Eq. (4) is represented as follows, using Eq. (10) and (11).

$$[PAN] = \frac{k_7 \cdot k_{14} \cdot k_{16}}{k_1 \cdot k_{15} \cdot k_{17}}[RCHO][OH] \ [O_3] \quad (12)$$

It can be understood by Eq. (12) that the concentration of PAN was proportional to O_3.

3.2. Low- and High-NO_X Regimes

For the Low-NO_X regime, the oxidation pathways for RH play a key role in O_3 production, due to the low artificial NO_X emission sources and the high levels of biogenic hydrocarbon from forests. Thus, in this system, higher RO_2 production resulting from active reaction of RH with OH, reaction (R2) produces HO_2 by reaction with NO, (R4). OH and RO_2 radicals therefore are lost mainly by reactions (R2) and (R4), and the dominant sink for Odd-H is reaction of HO_2, (R12). Hence, in the Low-NO_X regime, OH and RO_2 sinks may be ignored in Eq. (5). The resulting approximate solution for Eq. (5) is

$$2k_6[O_3] + B[RH] = 2k_{12}[HO_2]^2 \quad (13)$$

Thus, HO_2 concentration for the Low-NO_X regime from Eq. (13) is

$$[HO_2]_{Low-NO_X} = \left(\frac{2k_6[O_3] + B[RH]}{2k_{12}}\right)^{1/2} \quad (14)$$

OH concentration for the Low-NO_X regime is represented as follows from Eq. (7) and (14).

$$[OH]_{Low-NO_X} = \frac{k_5}{(2k_{12})^{1/2}} \cdot \frac{(2k_6[O_3] + B[RH])^{1/2} \cdot [NO]}{k_2[RH] + k_3[CO]} \quad (15)$$

$P(O_3)$ for the Low-NO_X regime is represented as follows from Eq. (8) and (15).

$$P(O_3)_{Low\text{-}NO_X} \sim \frac{k_5}{(2k_{12})^{1/2}} \cdot (2k_6[O_3] + B[RH])^{1/2} \cdot [NO] \quad (16)$$

Eq. (14) shows that HO_2 radical is proportional to RH but independent of NO_X. Eq. (15) shows that OH radical is proportional to NO_X but inversely-proportional to RH. Eq. (16) shows that O_3 production is proportional to NO_X but has a weak dependence on RH in the Low-NO_X regime.

For the High-NO_X regime, HO_2 and RO_2 radicals are lost mostly by reaction with NO, reactions (R4) and (R5), due to the large artificial NO_X emission sources. Hence, the dominant sink for Odd-H is formation of HNO_3, (R9). Thus, both HO_2 and RO_2 sink terms may be ignored in Eq. (5). The resulting approximate solution for Eq. (5) is

$$2k_6[O_3] + A[OH][RH] + B[RH] = k_9[OH][NO_2] \quad (17)$$

Thus, OH concentration for the High-NO_X regime from Eq. (17) is

$$[OH]_{High\text{-}NO_X} = \frac{2k_6[O_3] + B[RH]}{k_9[NO_2] - A[RH]} \quad (18)$$

HO_2 concentration for the High-NO_X regime is represented as follows from Eq. (7) and (18).

$$[HO_2]_{High\text{-}NO_X} = \frac{(2k_6[O_3] + B[RH]) \cdot (k_2[RH] + k_3[CO])}{k_5[NO] \cdot (k_9[NO_2] - A[RH])} \quad (19)$$

$P(O_3)$ for the High-NO_X regime is represented as follows from Eq. (8) and (19).

$$P(O_3)_{High\text{-}NO_X} \sim \frac{(2k_6[O_3] + B[RH]) \cdot (k_2[RH] + k_3[CO])}{k_9[NO_2] - A[RH]} \quad (20)$$

Eq. (18), (19), and (20) show that in the High-NO_X regime, OH and HO_2 radicals concentrations and O_3 production are proportional to RH but inversely- proportional to NO_X.

4. Evaluation for the Osaka Bay and Surrounding Areas of Japan

4.1. Method

The Osaka Bay and surrounding areas of Japan (shown in Fig. 2) were evaluated by three-dimensional simulation using CBM-IV[3] photochemical mechanism, in order to distinguish the Low- and High-NO_X regimes. The black points in Fig. 2 represented the 106 monitoring stations of ambient air pollutants and meteorological conditions in Hyogo and Osaka of the simulation area. Based on the result of the hierarchical cluster analysis[18] of observed O_3 concentrations for the typical summer days in the month of August from 1991 to 1995 at the 106 ambient air pollutants monitoring stations, Harima (36 km × 28 km), Hanshin (32 km × 32 km), and Osaka areas (28 km × 36 km) were selected[7]. The spatial mean values of predicted results for these 3 areas were used to evaluate the Low- and High-NO_X regimes in this study.

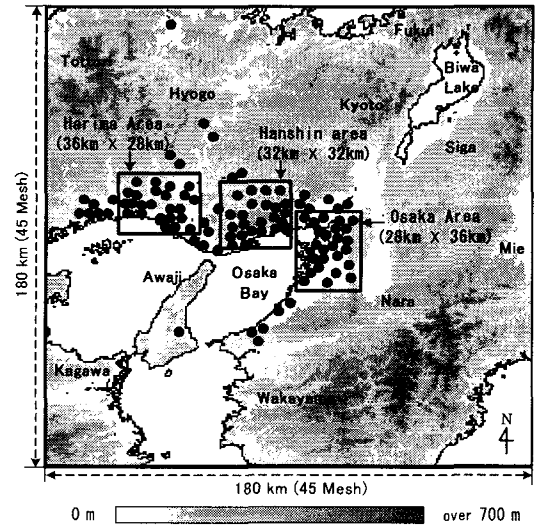

Fig. 2. Site location and horizontal simulation area of the Osaka Bay and surrounding areas. The points (●) represented the 106 monitoring stations.

The meteorological conditions and air quality were simulated for the typical summer day of fair weather with clear skies when photochemical reactions generating oxidants were significantly active, because it was purposed to investigate the atmospheric photochemistry for the typical summer day in the simulation area. Initial and boundary conditions of the simulations in this study were set according to Kondo[19] and Kondo *et al.*[20]. The calculations were started at 0900 LST of the first day, and carried out for a period of 48 hours. In this study, only results in the vertical third mesh 20 m as a ground-level from the second simulated day were discussed, when a diurnal cycle of chemistry, diffusion, advection, and pollutants concentrations were steady state, and the initial concentrations in the model domain no longer influenced the results.

NO_X and RH emission data estimated by Kondo *et al.*[20] in the simulation area were used. The amounts of NO_X and RH emissions from the anthropogenic sources were estimated 820 ton/day and 1200 ton/day in the whole simulation area, respectively. The amounts of NO_X and RH emissions for the Harima, Hanshin, and Osaka areas were shown in Table 1. The lower levels of NO_X and RH emission were showed in the Harima area, and the amounts of NO_X and RH emissions were estimated 25.4 [ton/day] and 154.7 [ton/day], respectively. The higher levels of NO_X and RH emissions were shown in the Hanshin and Osaka areas. The total amounts of NO_X and RH emissions from the anthropogenic sources in the Hanshin area were estimated 55.4 [ton/day] and 193.9 [ton/day], respectively. In the Osaka area, the total amounts of NO_X and RH emissions were estimated 64.3 [ton/day] and 276.3 [ton/day], respectively. In addition, RH/NO_X ratios for the Harima, Hanshin, and Osaka areas were 6.1, 3.5, and 4.3, respectively.

4.2. Evaluation for the Harima, Hanshin, and Osaka areas

The Harima area was estimated as a small-urban or a rural area with the lower emission levels, and the Hanshin and Osaka areas were estimated as an urban and a coastal area with the higher emission levels by Table 1 and previous researches[7,20]. In this study, the Harima, Hanshin, and Osaka areas in Fig. 2 were evaluated, in order to distinguish the Low- and High-NO_X regimes.

The A and B terms in Eq. (5) were empirically investigated by simulations for typical summer conditions in the Harima, Hanshin, and Osaka areas, and the results were shown in Table 2. Table 2 showed the values for A and B terms at 1200 LST, and also showed the literature values for the polluted rural areas of the United States by Sillman *et al.*[11] using the photochemical mechanism of Lurmann *et al.*[21]. The values in Table 2 showed similar order but different values, because each term depends on different primary pollutant emissions and meteorological conditions in simulation area and details of the used chemical mechanism. In addition, it was suggested that the values in the Harima area agreed reasonably well with the literature values due to rural conditions.

Table 1. The amounts of NO_X and RH emissions

	NO_X [ton/day]	RH [ton/day]	RH/NO_X
Harima	25.4	154.7	6.1
Hanshin	55.4	193.9	3.5
Osaka	64.3	276.3	4.3

Table 2. Typical values for A and B terms in Eq. (5) at 1200 LST

	A [$ppm^{-1} \cdot s^{-1}$]	B [$\times 10^{-6} \cdot s^{-1}$]
Osaka area	1.9	1.1
Hanshin area	2.0	1.1
Harima area	5.1	2.3
Sillman *et al.*[11,*]	4.9	3.0

*Literature values with the mechanism of Lurmann *et al.*[18] in polluted rural areas of the United States.

The Harima, Hanshin, and Osaka areas were evaluated with the Odd-H balance in Eq. (5). Fig. 3 showed the production and sink terms for Odd-H in Eq. (5) as a mean concentration from 1200 LST to 1500 LST for each area. For the Harima area, the simulation results suggested that the reaction rates of the OH and RO_2 sinks (P2, S1, and S3 in Fig. 3(a)) were relatively low, and the OH and RO_2 sink terms may be ignored in Eq. (5). It was suggested that Eq. (5) was rewritten as Eq. (13) for the Harima area. Thus, the Harima area may be defined the Low-NO_X regime. In contrary, for the Hanshin and Osaka areas, the simulation results suggested that the reaction rates of HO_2 and RO_2 sinks (S2 and S3 shown in Fig. 3(b) and (c)) were relatively low, and both HO_2 and RO_2 sink terms may be ignored in Eq. (5). It was suggested that Eq. (5) was rewritten as Eq. (17) for the Hanshin and Osaka areas. Thus, the Hanshin and Osaka areas may be defined the High-NO_X regime.

5. Conclusions

In this study, the atmospheric photochemistry of O_3-NO_X-RH were considered theoretically for the Low- and High-NO_X regimes. Equations of OH, HO_2, and production of O_3 as a function of NO_X and RH were represented. For the Low-NO_X regime, HO_2 radical is proportional to RH but independent of NO_X. OH radical is proportional to NO_X but in-

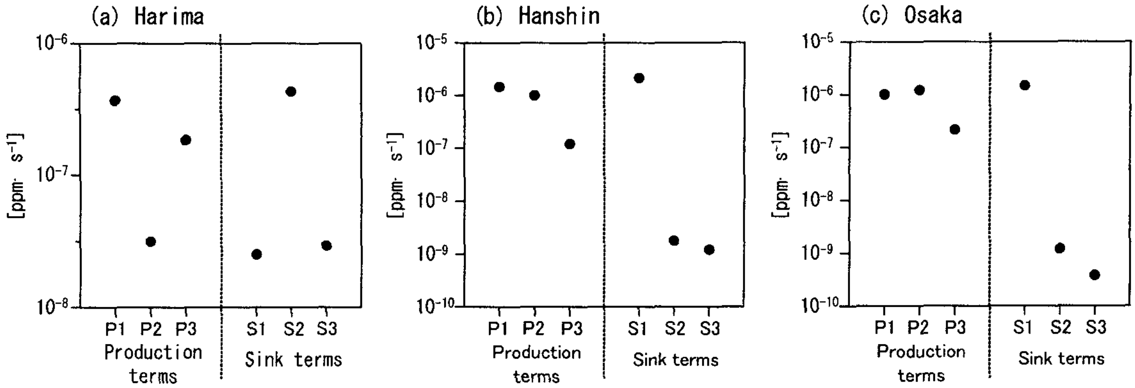

$$\text{Eq. (5)}\quad \underbrace{2k_6[O_3]}_{P1} + \underbrace{A[OH][RH]}_{P2} + \underbrace{B[RH]}_{P3} = \underbrace{k_9[OH]NO_2]}_{S1} + \underbrace{2k_{12}[HO_2]^2}_{S2} + \underbrace{2k_{13}[RO_2][HO_2]}_{S3}$$

Fig. 3. Production and sink values of Odd - H in each terms in Eq. (5) for (a) Harima, (b) Hanshin, and (c) Osaka areas. The values are mean concentrations from 1200 LST to 1500 LST.

versely-proportional to RH. O_3 production is proportional to NO_X but has a weak dependence on RH. For the High-NO_X regime, OH and HO_2 radicals concentrations and O_3 production are proportional to RH but inversely-proportional to NO_X. In addition, the Osaka Bay and surrounding areas of Japan were evaluated with the Odd-H balance by three-dimensional simulation. The simulation results showed that the reaction rates of the OH and RO_2 sinks were relatively low for the Harima area, and the reaction rates of HO_2 and RO_2 sinks were relatively low for the Hanshin and Osaka areas. Thus, it was suggested that the Harima area may be defined the Low-NO_X regime, and the Hanshin and Osaka areas, the High-NO_X regime.

Roselle and Schere[10], Sillman *et al.*[11], Milford *et al.*[12,13], and Sillman[14] researched the relationship between O_3 and its primary pollutant emissions in the United States, using a three-dimensional model. They reported that for the Low-NO_X regime, the process of O_3 formation is controlled almost entirely by NO_X and is largely independent of RH. On the other hand, O_3 production for the High-NO_X regime decreases with RH at higher NO_X emission levels, but a decrease in NO_X leads to an increase in levels of OH and peroxy-radicals (HO_2 and RO_2) and corresponds to increasing O_3. Their results also can be considered with equations in this study.

Therefore, the theoretical considerations of atmospheric photochemistry of O_3-NO_X-RH is needed to clarify the reasons for the different trends of between photochemical O_3 and its primary pollutants, and to suggest the balanced reduction policy of NO_X and RH emissions for decrease in O_3 concentration.

Acknowledgments

This work was funded by the Korea Meteorological Administration Research and Development Program under Grant CATER 2006-1101.

References

1) Dennis, R. L. and M. W. Downton, 1984, Evaluation of urban photochemical models for regulatory use, Atmos. Environ., 18, 2055-2069.
2) Dodge, M. C., 1989, A comparison of three photochemical oxidant mechanisms, J. Geophys. Res., 94, 5121-5136.
3) Gery, M. W., G. Z. Whitten, J. P. Killus and M. C. Dodge, 1989, A photochemical kinetics mechanism for urban and regional scale computer modeling, J. Geophys. Res., 94, 12925-12956.
4) Derwent, R. G., 1990, Evaluation of a number of chemical mechanisms for their application in models describing the formation of photochemical ozone in EUROPE, Atmos. Environ., 24, 2615-2624.

5) Ohara, T., S. Wakamatsu, I. Uno, T. Ando, S. Izumikawa, A. Kannari and Y. Tonooka, 1997, Development and validation of numerical model for photochemical oxidants, J. Japan Soc. Atmos. Environ., 32, 6-28.
6) Svensson, G., 1996b, A numerical model for chemical and meteorological process in the atmospheric boundary layer, Part. II: A case study of the air quality situation in Athens, Greece, J. Appl. Meteor., 35, 955-973.
7) Kim, D. Y., K. Yamaguchi, A. Kondo and S. Soda, 2001, Study on relationship between photochemical oxidant and primary pollutants emission amounts in Osaka and Hyogo regions, J. Japan Soc. Atmos. Environ., 36, 156-165.
8) Kleinman, L. I., 1991, Seasonal dependence of boundary layer peroxide concentration: The low and high NO_X regimes, J. Geophys. Res., 96, 20721-20734.
9) Kleinman, L. I., 1994, Low and high-NO_X tropospheric photochemistry, J. Geophys. Res., 99, 16831-16838.
10) Roselle, S. J. and K. L. Schere, 1995, Modeled response of photochemical oxidants to systematic reductions in anthropogenic volatile organic compound and NO_X emissions, J. Geophys. Res., 100, 22929-22941.
11) Sillman, S., J. A. Logan and S. C. Wofsy, 1990, The sensitivity of ozone to nitrogen oxides and hydrocarbons in regional ozone episodes, J. Geophys. Res., 95, 1837-1851.
12) Milford, J., A. G. Russell and G. J. McRae, 1989, A new approach to photochemical pollution control, Implications of spatial patterns in pollutant responses to reductions in nitrogen oxides and reactive organic gas emissions, Environ. Sci. Tech., 23, 1290-1301.
13) Milford, J., D. Gao, S. Sillman, P. Blossey and A. G. Russell, 1994, Total reactive nitrogen (NO_y) as an indicator of the sensitivity of ozone to reductions in hydrocarbon and NO_X emissions, J. Geophys. Res., 99, 3533-3542.
14) Sillman, S., 1999, The relation between ozone, NO_X and hydrocarbons in urban and polluted rural environments, Atmos. Environ., 33, 1821-1845.
15) Atkinson, R., 1986, Kinetics and mechanisms of the gas-phase reactions of the hydroxyl radical with organic compounds under atmospheric conditions, Chem. Rev., 86, 69-201.
16) Kleinman, L. I., 1986, Photochemical formation of peroxides in the boundary layer, J. Geophys. Res., 91, 10889-10904.
17) Cox, R. A. and M. J. Roffey, 1977, Thermal decomposition of peroxyacetylnitrate in the presence of nitric oxide, Environ. Sci. Tech., 11, 900-906.
18) Rodeghier, M., 1996, Surveys with Confidence: A Practical Guide to Survey Research Using SPSS, SPSS Inc.
19) Kondo, A., 1999, Study on development and application of numerical simulation model to urban atmospheric environmental conservation, A Thesis Submitted to the Graduate School of Engineering at Osaka University, Japan.
20) Kondo, A., K. Yamaguchi, E. Nishikawa, T. Hara and R. Okazaki, 1999, Influence of ship emission on atmospheric pollutants concentration around Osaka Bay area, J. Kansai Soc. Naval Arch., 231, 101-109.
21) Lurmann, F. W., A. C. Lloyd and R. Atkinson, 1986, A chemical mechanism for use in long-range transport / acid deposition computer modeling, J. Geophys. Res., 91, 10905-10936.